JOURNAL OF VIROLOGY, Sept. 2000, p. 8614–8622 Vol. 74, No. 18
0022-538X/00/$04.00+0

Follicular Dendritic Cells and Dissemination of Creutzfeldt-Jakob Disease

LAURA MANUELIDIS,[1]* IGOR ZAITSEV,[1] PANDELAKIS KONI,[2]† ZHI YUN LU,[1] RICHARD A. FLAVELL,[2,3] AND WILLIAM FRITCH[1]

Section of Neuropathology,[1] Section of Immunobiology,[2] and Howard Hughes Medical Institute,[3] Yale University School of Medicine, New Haven, Connecticut 06520

Received 1 May 2000/Accepted 12 June 2000

The contribution of immune system cells to the propagation of transmissible encephalopathies is not well understood. To determine how follicular dendritic cells (FDC) may act, we challenged lymphotoxin β null and wild-type (wt) controls with a Creutzfeldt-Jakob disease (CJD) agent. There was only a small difference in incubation time to clinical disease even after peripheral challenge with low infectious doses (31 in a total of 410 days). Brain pathology with extensive microglial infiltration, identified by keratan sulfate, as well as astrocytic hypertrophy, was also equivalent in all groups despite the fact that null mice had neither FDC nor splenic metallophilic macrophages that filter particulate antigen. Because FDC accumulate pathologic prion protein (PrP) in infected but not wt mice, we studied the cellular distribution of PrP by confocal microscopy. The majority of pathologic PrP collected on the plasma membrane of FDC, as identified by the Ca^{+2}-binding protein S100A. This surface distribution suggested that agent aggregated with pathologic PrP might spread by cell-to-cell contacts. While several types of leukocytes may be involved in agent dissemination, cells of myeloid lineage were found to be infectious. Moreover, perivascular tracks of microglia and abnormal PrP after intraperitoneal inoculation were consistent with hematogenous spread. In summary, FDC are not required for CJD agent spread from the periphery, although FDC may enhance spread through surface accumulation of pathologic PrP. While it is still not clear where the infectious agent replicates, macrophages can sequester appreciable levels of infectivity and hence act as reservoirs for prolonged latent infection.

The role of the immune system in transmissible encephalopathies was discounted for many years (4, 11, 32). While immune responses typical for acute viral infections do not occur in this group of diseases, it has become increasingly apparent that cells of the immune system (i) participate in clearance of the infectious agent at entry sites of infection, (ii) supply routes for agent spread, and (iii) can themselves provide fertile ground for agent replication or accumulation. In addition to these critical initial events at the periphery, macrophage-derived microglia of the brain can be central players in an autoinflammatory process that incites progressive neurodegenerative and amyloid changes (1, 25).

The emergence of bovine spongiform encephalopathy has renewed interest in the role of immune system cells during natural and experimental infections originating from peripheral sites. Early studies with mouse-adapted scrapie inoculated subcutaneously showed that the infectious agent seeded the spleen, was rapidly cleared, and then began to reappear, replicating in spleen and later spreading to lymph nodes and the central nervous system (CNS) (9). Subsequent studies demonstrated the infectious agent associated with circulating white blood cells in both experimental and natural Creutzfeldt-Jakob disease (CJD), implicating the vascular system as a conduit for agent spread both into and out of the brain (26, 27, 35). Nevertheless, particular agent strains can have very different degrees of lymphotropism and neurotropism. For example, unlike scrapie, transmissible mink encephalopathy revealed "extremely limited replication of the virus in lymphatic organs," and detectable spleen infectivity was found only after agent accumulated in the brain (12). Different agent strains may also target distinct classes of bone-marrow-derived or other lymphoreticular cells. Thus, to delineate common versus more specialized agent strategies, it is necessary to evaluate several independent strains of agent.

When spleen cells are fractionated by class, all cell types (B cells, T cells and, to a lesser extent, macrophages) have displayed appreciable levels of infectivity, despite the paucity of prion protein (PrP) expression by these cells (8, 20, 34). PrP has been linked to infection and disease progression because the scrapie agent is unable to replicate in PrP knockout mice (7), and when PrP levels are increased by insertion of multiple PrP gene copies the disease progresses more rapidly (33). The high levels of infectivity in spleen cells expressing little PrP is, therefore, somewhat paradoxical, and remarkably >1,000-fold overexpression of PrP in lymphocytes does not increase the infectious titer in the spleen (34). Nevertheless, because pathologic PrP can accumulate in spatial association with follicular dendritic cells (FDC), a highly specialized immobile cell in the germinal centers of secondary lymphoid organs, some investigators have postulated FDC are required for agent replication (6, 16). If this were true, removal of FDC should abolish or severely limit agent replication, and hence agent spread to the CNS. An alternate possibility is that FDC are interacting accumulators of agent that may aggregate together with PrP. In this capacity, FDC may collect infectivity from and transmit it to white blood cells trafficking between peripheral sites and the brain. Since FDC are very difficult to isolate or culture (15), transgenic and other molecular strategies can be used to find if FDC are essential for propagating or spreading infection.

The recently developed lymphotoxin β-deficient mice ($LT\beta^{-/-}$) lack FDC in secondary lymphoid organs but have functional B and T cells (19). These mice have mesenteric and

* Corresponding author. Mailing address: Section of Neuropathology, Yale University School of Medicine, 310 Cedar St., New Haven, CT 06510. Phone: (203) 785-4442. Fax: (203) 785-6381. E-mail: laura.manuelidis@yale.edu.

† Present address: Medical College of Georgia, Augusta, GA 30912.

cervical lymph nodes in contrast to LTα$^{-/-}$ mice that are also FDC null. LTβ$^{-/-}$ mice are also useful for comparison to tumor necrosis factor receptor (TNFR) I knockouts lacking FDC because lymphotoxin and TNF cytokines act through different intracellular domains that can mediate independent sets of cellular and tissue responses. Indeed, the LTβ receptor is expressed on stromal cells in various lymphoid tissues, while TNFRs I and II are expressed very broadly (10). Additionally, LTβ$^{-/-}$ mice lack the MOMA-1+ metallophilic macrophages of the marginal zone thought to be involved in antigen and cellular trafficking between hematogenous and lymphatic circulations. We show here that a strain of CJD can propagate and cause clinical disease in LTβ$^{-/-}$ mice, even when inoculated at very low to limiting dilutions intraperitoneally (i.p.). These mice showed only a very small increase in incubation time compared to wild-type (wt) controls. Thus, FDC are not essential for CJD agent replication peripherally nor are they required for spreading infection. Instead, the data suggest that FDC can enhance dissemination and/or diminish clearance of the CJD agent.

To investigate how FDC might disseminate agent to migrating cells, we evaluated plasma membranes of infected wt mice by confocal microscopy. Only infected mice (but not normal or LTβ$^{-/-}$ mice) showed obvious pathologic PrP in the spleen, and the abnormal PrP accumulated at the surface of FDC. These PrP-rich membranes also formed an intimate reticular network surrounding small lymphocytes, giving them the ability to transfer membrane-bound or trapped infectious agent to developing and exiting cells. Furthermore, bursts of aggregated PrP around vessels in the cerebrum after peripheral inoculation also suggested that at least some agent could be seeded from cells trafficking into the brain from the bloodstream. While the exact types of white blood cells involved in agent replication and transfer are still not entirely clear, our assays suggest that macrophage-derived cells can participate in repeated cycles of agent clearance and dissemination.

MATERIALS AND METHODS

Mice. LTβ$^{-/-}$ mice were from expanded from original littermates of the transgenic (Tg) line and verified by PCR as previously described (19). These Tg and background wt [(C57BL/6 × 129)F_2] controls were kept under specific-pathogen-free conditions in the CJD facility; LTβ$^{-/-}$ mice were additionally maintained on Sulfatrim to prevent infection. A more virulent strain of CJD, designated FU (21) and also known as Fukuoka-2, (16, 36), was used for the present experiments. Frozen passaged whole-brain homogenates (untreated with heat or detergent) from clinically ill CD-1 mice were used to inoculate CD-1, Tg, and wt mice intracerebrally (i.c.) (25 to 30 μl) or i.p. (100 μl), and each group contained six to nine mice. The inoculum was also titered i.c. in CD-1 mice by serial dilution. For reference, the dose inoculated represents the i.c. infectious units (IU) assayed in CD-1 mice, and the i.p. lethal dose was empirically determined. CD-1 mice are also used as an additional reference point because the wt controls for the LTβ$^{-/-}$ mice as well as purebred C57BL/6 mice also showed somewhat longer incubations after i.c. challenge than CD-1 mice (L. Manuelidis and W. Fritch, unpublished data). Because we have also observed that inocula can lose titer with storage at −70°C, all experimental mice were bred to be 6 to 8 weeks of age on the same day for inoculation. Three of the paired Tg-wt groups were inoculated with the identical homogenate dilution mixes (i.c., 50 IU; i.p., 2,000 IU; and i.p., 20 IU) on the same day. The fourth pair group (i.c., 3 IU) was inoculated later with a dilution of a different FU homogenate stock.

Tissue processing and controls. Mice were killed by an overdose of sodium pentobarbital when CJD had progressed clinically to a terminal stage, or at the designated end of the experiment (586 days postinoculation, equivalent to an age of ~635 days). Complete autopsies were done, and half brains were frozen for later Western-blotting studies. For microscopic evaluation, brain, spleen and, where possible, lymph nodes and thymus were fixed in 10% formalin and embedded in paraffin. As expected, fewer lymph nodes were obtained in LTβ$^{-/-}$ mice because of the effect of this mutation on peripheral lymph nodes as previously documented (19). Sectioning and staining with primary antibodies to keratin sulfate, PrP, and glial fibrillary acidic protein (GFAP) with reagents and methods were as previously described (25). As in previous experiments, several controls were included. Citrate autoclaving was used to specifically expose and limit detection to pathologic PrP. Using this antibody, pathologic PrP was not detected on LTβ$^{-/-}$ secondary lymphoid organs and also was not detectable in any organs of uninfected wt or CD-1 (Swiss) mice with the exception of pancreatic islet cells. (Western blotting of fresh pancreatic islet cells also yielded a strong PrP-like band [K. Radebold, I. Zaitsev, and L. Manuelidis [unpublished observations].) All PrP immunohistochemistry experiments also included comparably fixed CD-1 spleens from normal and CJD-infected mice of various ages (10 to 100 weeks old). Furthermore, spleen paraffin blocks contained endstage FU brain (LTβ$^{-/-}$, wt, and CD-1) as a positive internal control for PrP or as a negative control for glial fibrillary acidic protein staining.

Several modifications of tissue treatment were also done to further evaluate PrP resistance in infected mice and to understand the cellular compartments involved in abnormal PrP collection. Formic acid treatment (85% for 40 min) of formalin-fixed tissue sections before autoclaving enhanced PrP differentiation inconsistently and on thinner, 4-μm sections PrP could be reduced, as assessed by signal intensity after 3 min of alkaline phosphatase development. To further understand the distribution of pathologic PrP on FDC, additional control studies included tissues from CD-1 mice (normal and CJD brain injected peripherally) that were perfused with 4% paraformaldehyde in buffer A (29). This fixation, followed by autoclaving, enhanced the detection PrP on many cell processes that were not as abundant in the formalin-fixed spleen. A similar extensive reticular pattern of PrP staining (albeit with less cytological detail) was seen in acetone-fixed frozen and autoclaved sections, further validating the results found with perfusion. FDC were also defined in adjacent sections with antibodies to the Ca^{+2}-binding protein S-100A (37), and tissue sections were treated with 0.1% trypsin for 20 min to unmask this antigen. Antibodies were detected using ABC with Vector red development (Vector Labs), followed by light hematoxylin counterstaining. Confocal microscopy sectioning (Vector red is strongly fluorescent using filters with excitation and emission characteristics for Texas red) and three-dimensional analysis were done as described using a Leica confocal microscope with a pizoelectric *z*-axis stepper and a continuously adjustable pinhole (22).

Western blotting for the more protease-resistant portion of PrP (PrP-res) was done on blots of lysed unfractionated brain homogenates digested with proteinase K, and chemiluminescence detection protocols were followed as described in detail elsewhere (24). The digestion conditions were chosen based on a complete absence of PrP-res in several normal mouse brain homogenates. The rabbit polyclonal antibody here used for both microscopic detection and Western blots has shown high sensitivity for rat and mouse PrP and highlights the same PrP bands as antibodies to conserved PrP peptides (21, 25). After PrP detection, the blots were stripped and reprobed with a mouse antibody to tubulin (Sigma) at a 1:2,000 dilution to determine relative protein loads and optimal digestion of samples. Secondary anti-mouse and anti-rabbit peroxidase antibodies were from Amersham.

RESULTS

It was important to chose an informative strain of CJD and to determine the dose most likely to bring out differences in the LTβ$^{-/-}$ compared to the wt [(C57BL/6 × 129)F_2] mice. When using an i.p. or other peripheral route of infection, incubation times are always markedly extended compared to those found after i.c. challenge, and thus it is critical to determine the limiting i.p. dose. Second, pathologic changes can be subtle after peripheral infection compared to the massive pathologic changes elicited by lower i.c. doses (28). Third, common CJD agents isolated and propagated here from typical patients in the United States have a low virulence for outbred and inbred mice (30). We therefore we used a more virulent CJD agent isolated in Asia, designated FU, that causes obvious clinical symptoms as well as a more rapidly progressive disease in mice (21, 36). FU also elicits widespread spongiform change and distinctive amyloid deposits in brain after i.c. inoculation of CD-1 mice.

To determine whether dilution of this strain was itself sufficient to alter clinical symptoms or pathology after peripheral inoculation, we tested standard outbred CD-1 mice used for passage. Peripheral inoculation of 200,000 and 20,000 i.c. IU yielded unambiguous clinical disease using an i.p. route. Days to terminal disease were 230.7 ± 4.7 (standard error of the mean) and 298.3 ± 14.5, respectively. We also used an intravenous (i.v.) route to rule out possible incubation effects from direct infection of nerves during i.p. puncture. In this case a similar dose (~1/3 of the above IU) was delivered i.v. These i.v.-inoculated mice also showed clear clinical symptoms and

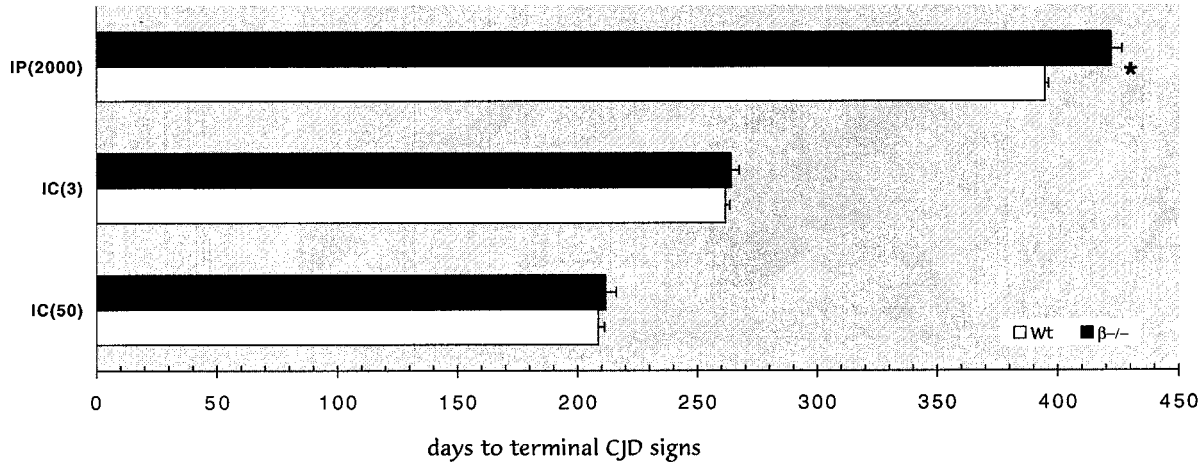

FIG. 1. Graph of incubation time to terminal disease for wt control [(C57BL/6 × 129)F_2] (open bars) and LTβ$^{-/-}$ (filled bars) mice inoculated with FU on the same day with the same mixture. The *y* axis shows the route and infectious dose (in IU [in parentheses]) for each pair. Only the i.p. route at low infectious dose shows a small difference between wt and LTβ$^{-/-}$ mice (statistical significance, $P < 0.0001$, is noted by an asterisk with the standard error of the mean (SEM) as indicated on each bar; the Student *t* test and ANOVA yielded the same *P* value).

similar pathology at comparable times of 239.2 ± 5.4 and 314.6 ± 16.7 days, respectively. The reasonably tight and similar numbers with the higher dose in both the i.p. and i.v. groups indicate a direct neural route of infection was unlikely with our i.p. inoculations. The increasing mouse-to-mouse variability in incubation time with the next serial dilution (20,000 IU) also suggested an endpoint would be reached within the next 1- to 2-log dilution. Indeed, in CD-1 mice inoculated with 2,000 IU i.p. there were no mice (total = 12) that showed clinical symptoms. Most of the mice died "spontaneously" between 305 and 380 days (345.5 ± 12), a time consistent with death from CJD, but one that could not be proven histologically in these instances. However, in accord with this interpretation, 2 of 12 of the asymptomatic mice that had been randomly sacrificed before death (at 287 and 390 days) showed widespread spongiform and PrP amyloid changes in the brain. These lesions were comparable to those seen after i.c. inoculations. In summary, these experiments (i) empirically defined low-dose FU infectivity for peripheral routes; (ii) showed that immune system defects were not required for prolonged asymptomatic disease as had been proposed in scrapie (17); (iii) gave comparable effects when infected by i.v. and i.p. routes, implicating comparable non-neural pathways of agent spread; and (iv) indicated that brain pathology induced by this CJD strain were not modified by agent dilution or route of inoculation. The latter feature was important subsequently for the correct evaluation of apparently resistant (asymptomatic) LTβ$^{-/-}$ mice inoculated with limiting doses of FU delivered i.p.

The same stock of FU homogenate was used for simultaneously challenging wt [(C57BL/6 × 129)F_2] and LTβ$^{-/-}$ mice by the i.c. and i.p. routes. Because the effects of severe genetic immunodeficiency can be inapparent using inocula with high infectious titers (5), we sought to bring out any possible effects of absent FDC by using low and limiting doses of FU for each respective route (i.c. and i.p.). Figure 1 shows that low and limiting doses gave comparable incubation times after i.c. inoculation in wt and LTβ$^{-/-}$ mice at both low (50 IU) and limiting (3 IU) doses. When analyzed statistically, wt and LTβ$^{-/-}$ mice showed no significant differences ($P = 0.84$ and 0.58, respectively). All i.c. inoculated mice displayed typical clinical signs of CJD in the same time range with a <3-day difference in either i.c. pair. Additionally, the mean periods from the start of clinical signs to terminal-stage disease were similar (11.7 and 15.7 days, respectively). Figure 1 also shows corresponding groups of wt and LTβ$^{-/-}$ mice inoculated i.p. on the same day with the same homogenate mixture. All mice in both pair groups showed typical clinical signs of CJD and the mean duration of symptoms was comparable to that seen with i.c. inoculation (15.7 and 11.6, days respectively). There was, however, a small increase of ~29 days to clinical or terminal disease in the LTβ$^{-/-}$ mice inoculated i.p. This difference was apparent even at these low doses because the incubation time was well defined numerically and confined to a relatively narrow range (≤28 days). This difference was statistically significant ($P < 0.0001$) as determined by both Student's *t* test and analysis of variance (ANOVA). Thus, FDC have a small incubation effect in this model of CJD but are not required for dissemination of infectivity after peripheral infection. This interpretation was further supported in an additional group of mice inoculated on the same day with a more dilute suspension of FU (Table 1). Only at these limiting doses did clinical symptoms disappear in LTβ$^{-/-}$ mice compared to the wt controls. Even at these very low doses, "resistance" to the agent was equivocal, and the LTβ$^{-/-}$ mice were comparable to nontransgenic CD-1 mice challenged i.p. at limiting CD-1 doses.

Histologic and immunochemical studies of brain also confirmed obvious lesions in LTβ$^{-/-}$ mice inoculated i.p. with 2,000 IU. These were indistinguishable from lesions seen in CD-1 and wt mice inoculated i.c. or i.p., and there was widespread involvement of the cerebrum. Figure 2A to C shows three adjacent sections from a prototypic LTβ$^{-/-}$ mouse in this i.p.-inoculated group. There are small deposits of PrP amyloid (A), a more extensive network of infiltrating activated microglia detected with antibodies to keratan sulfate (B), and intense astroglial (GFAP) hypertrophy (C) in this region. The intensity of GFAP staining also highlights the widespread spongiform changes even at this low magnification. Positively scored mice at limiting doses (Table 1) had comparable lesions. Uninfected mice did not show these changes. Additionally, even older nondiseased mice inoculated with FU i.p. at limiting doses and sacrificed at 586 days (Table 1, mice marked "586") did not show these changes. Adjacent sections from one of these aged but healthy representative LTβ$^{-/-}$ mice are

TABLE 1. Limiting i.p. doses for wt and LTβ$^{-/-}$ mice, indicating days to clinical signs and terminal disease[a]

Mouse type (dose [IU])	Mouse no.	CJD score	No. of days to[b]:		No. of days sick
			Signs	Terminal	
wt (20)[c]	1	Yes	391	405	14
	2	Yes	413	433	20
	3	Yes	424	440	16
	4	Yes	424	440	16
	5	Yes	395	405	10
	6	Yes	412	426	14
	7	Yes	412	426	14
LTβ$^{-/-}$ (20)	1	?		455 (FD)	
	2	Yes		455 (SC)	
	3	Yes	470	482	12
	4	?		561 (FD)	
	5	N		"586"	
	6	N	(Lymphoma)	"586"	
	7	N	(Lymphoma)	"586"	

[a] CJD were scored as "Yes" for obvious CJD signs and PrP-res pathology. Probable clinical signs are scored as "?," and "N" means the animal was negative for both CJD signs and brain lesions. FD, animals were found dead; SC, animals were sacrificed for pathology evaluation (without clear signs); "586", arbitrary end day of the experiment. The number of days sick is not applicable to these categories and so are left blank.

[b] Signs, animal first showed clinical signs of disease, such as slowness and hunching. Terminal is moribund animal.

[c] The mean number of days to showing signs of disease and to death were 410.1 ± 4.9 (SEM) and 425.0 ± 5.6, respectively, for wt mice. The mean number of days sick was 14.9 ± 1.1.

shown for comparison in panels D to F. Note that no pathologic PrP was detected (D) and that microglial and astrocyte activation is minimal (E and F, respectively). Because 10^6 IU of agent can be present in a gram of brain without detectable PrP changes (24), it is not known if these remaining mice harbored the infectious agent in their brains.

Western blotting was used to evaluate PrP pathology on a more quantitative basis. PrP-res was developed under conditions where PrP of uninfected mice is completely digested with proteinase K (PK; see Materials and Methods). Conditions that abolished PrP in normal mice (21) also reproducibly digested most tubulin. Thus, as an internal control for PK digestion of normal protein (including PrP), blots were first exposed to PrP antibody and were subsequently probed with an antibody to 50-kDa tubulin. This approach also clarified relative lane loads in undigested homogenates. Figure 3 shows a representative sampling of wt and LTβ$^{-/-}$ mice (lanes wt and −/−, respectively) inoculated i.p. or i.c. as indicated. Brain homogenates from i.p.-infected mice that were digested with PK to resolve PrP-res are shown in lanes 1 to 6. Note that tubulin is digested (A) but that PrP-res bands at 28, 26, and 19 kDa are present (B). For comparison, equal portions of the same series of homogenates, not subjected to PK digestion, were electrophoresed in lanes 10 to 15. Tubulin at 50 kDa is intact, and PrP in these undigested sample lanes show higher-molecular-weight PrP bands. Moreover, minor differences in PrP-res intensity among each of these samples corresponded to minor differences in sample loads rather than to substantial differences in the amount of PrP-res. For example, the positive LTβ$^{-/-}$ mouse homogenate in lanes 6 and 15 contained less material than adjacent homogenates. Repeat blots with slight adjustments of sample load confirmed this interpretation, and all mice showing histologic changes gave obvious PrP-res bands.

Spleen and lymph nodes from CD-1, wt, and LTβ$^{-/-}$ mice were also examined. FDC-like cells were positive for pathologic PrP in germinal centers of spleen in infected CD-1 and wt mice, whereas mock-infected mice showed no PrP reactivity on FDC with our antibody. Infected mice also showed obvious PrP-positive FDC-like cells in lymph nodes, as depicted in a representative low-power micrograph from a mouse inoculated i.p. with 2,000 IU (Fig. 2G). In contrast, all spleens and all sampled lymph nodes from LTβ$^{-/-}$ mice failed to show any similar PrP staining, as representatively shown in Fig. 2H. Furthermore, the spleen had a disorganized lymphoid structure without germinal centers, as previously described (19). These analyses verified that these sick mice had been accurately genotyped and lacked FDC.

The similarly uniform incubation time in LTβ$^{-/-}$ compared to wt mice inoculated with low doses i.p. and the widely distributed lesions in the cerebral cortex made it likely that the CJD agent was, at least in part, spreading to the CNS by a hematogenous route. The detection of CJD infectivity in buffy coat cells (cf. the introduction) furthers this possibility. Additionally, profound and widespread deposition of pathologic PrP in many small vessels at early stages of infection in a very prolonged rat CJD model had suggested infection could be carried by white blood cells penetrating the blood-brain barrier (4). However, because inoculation of those rats was by an i.c. route, direct spread from adjacent brain parenchyma could not be ruled out. In the present experiments i.p. inoculation also led to the accumulation of pathologic PrP around vessel walls in both wt and LTβ$^{-/-}$ mice (Fig. 2I and J, respectively). The burst of PrP aggregates emanating from several small thin-walled vessels, as shown at arrows in panel I, are particularly compatible with footprints from an invading agent. On higher-power examination, using double labeling to detect both pathologic PrP and keratan sulfate, PrP was found beneath the endothelium and within adjacent microglial cells, a macrophage-derived cell type that can migrate into and out of the brain from the bloodstream.

It was important to find if myeloid cells are capable of harboring the infectious agent, especially at a time when they could have the most impact on agent spread. To clarify the role of myeloid cells in infection, we have been evaluating fresh and cultured spleen macrophages. Briefly, adherent cells with a dendritic to macrophage morphology are cultured for 5 weeks so that any dead and dying B- and T-cell fragments should be washed away. After 5 weeks in vitro, cultured cells took up fluorescent beads and were >95% positive for Mac3, CD45, and CD11b by fluorescence-activated cell sorter (FACS) analysis (M. Brock and L. Manuelidis, unpublished data). For infectivity assays, cultured macrophages were pooled from two spleens of CD-1 mice inoculated i.p. 54 days earlier with low doses of FU. This time point represents a relevant early period in the course of infection, given the >300 days needed to develop CJD. It also corresponds to a time of high scrapie infectivity in the spleen but not in the brain (9). One aliquot of living cells was processed to confirm the typical FACS characteristics, while the second aliquot was tested for infectivity by i.c. injection. All seven recipient mice inoculated with ~10^5 viable macrophages showed clear signs of CJD at 182.7 ± 2.3 days. Because infectivity of viable cells may not be strictly comparable to disrupted material, the IU value cannot be calculated precisely. Nevertheless, propagated spleen macrophages were able to retain and transmit appreciable FU infectivity before the agent had established itself in the brain. Alternate interpretations are that the few fibroblasts or inapparent residual lymphocytes retained infectivity. However, infection of mice with other agent strains, using different methods for macrophage isolation, have also revealed significant

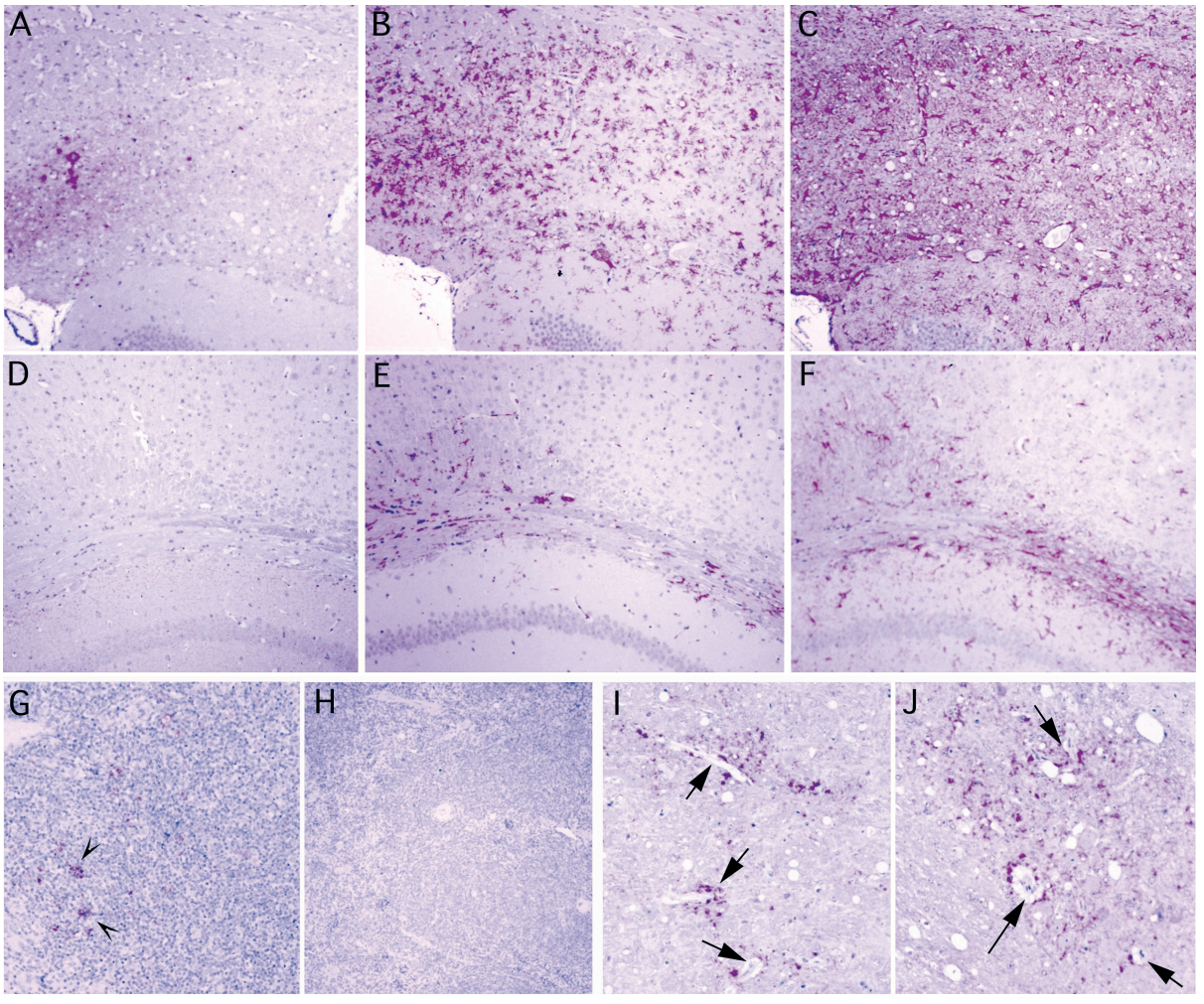

FIG. 2. Lesions in representative LTβ$^{-/-}$ mouse inoculated i.p. at low dose (2,000 IU) are shown in panels A to C. Adjacent cerebral sections show focal deposits of pathologic PrP (red) in a region with spongiform change (A), even more abundant accumulating microglia (red) stained for keratan sulfate (B), and extreme hypertrophy of GFAP-positive astrocytes (C). An aged LTβ$^{-/-}$ mouse, scored as negative after i.p. inoculation with a limiting dose (20 IU; see Table 1), is shown as a control in panels D through F. Note the absence of pathologic PrP (D), the paucity of infiltrating microglia (E), and the lack of gliosis (F) in comparable cerebral sections from these very old mice. Panel G shows abnormal PrP in FDC-like cells of a wt lymph node (inoculated i.p.) fixed in formalin at 398 days, whereas panel H demonstrates the absence of PrP staining in LTβ$^{-/-}$ mouse spleen at 424 days after i.p. inoculation. (I and J) Vessels in the brain of wt and LTβ$^{-/-}$ mice after i.p. inoculation. Asymmetric bursts of abnormal PrP are seen around small, thin-walled vessels (arrows, panel I) of a wt mouse, and PrP also surrounds and follows vessels in the i.p.-inoculated LTβ$^{-/-}$ mouse (J). All panels were hematoxylin counterstained.

infectivity in splenic macrophages at terminal stages of disease (20, 34). Thus, it is more likely that the infectivity assayed here was sequestered in macrophages.

On the basis of the above results, the somewhat faster demise in wt compared to LTβ$^{-/-}$ mice inoculated i.p. might entail either of two pathways. First, a lack of metallophilic macrophages that filter particulate antigen might lead to poor capture of the inoculated agent in LTβ$^{-/-}$ mice. Alternatively or additionally, FDC might enhance agent spread through physical contact with other infected lymphocytes (and specific cells of myeloid lineage). FDC may initially trap the CJD agent through a non-antibody-dependent (membrane-mediated) interaction and subsequently re-exchange the agent with circulating lymphocytes for dissemination. In contrast, when FDC are absent, macrophages ingest and partially inactivate apoptotic but infectious lymphocyte fragments, more effectively removing agent from the circulation. One prediction of this model would be the identification of aggregates of abnormal PrP on the surface of FDC. Such aggregates often trap and sequester the infectious agent in CJD (31), and on the surface of FDC they could facilitate the donation of agent to groups of closely associated lymphocytes. Such aggregates would roughly parallel antigen-antibody complexes with trapped virus on the surface of FDC, such as those known to seed human immunodeficiency virus.

To determine if abnormal PrP was concentrated on the plasma membrane of FDC, we perfused mice with paraformaldehyde for confocal microscopy. Compared with frozen sections, this approach preserved structure, limited the artifactual diffusion of molecules, and additionally enhanced detection of pathologic PrP (see Materials and Methods). However, the typical antibodies used to rigorously identify FDC were poorly reactive in tissue optimally preserved for structure. Thus, we used antibodies to S-100A, a marker of differential calcium capture that has been recently been reported to define FDC in germinal centers for electron microscopy (37). In formalin-fixed tissue, LTβ$^{-/-}$ mice showed no positive cells in the disorganized lymphoid zone, whereas wt mice displayed S-100

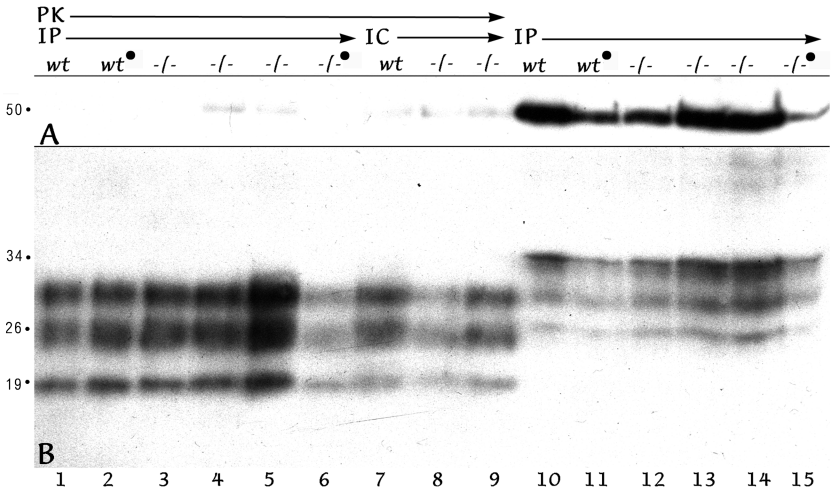

FIG. 3. Western blot of representative mouse brains from mice inoculated i.p. (IP lanes) or i.c. (IC lanes). The mouse genotype is indicated as wt or −/− (for LTβ$^{-/-}$), and a filled circle designates that the dose was limiting. The A panel shows that tubulin at 50 kDa after PK treatment is markedly reduced (lanes 1 to 9) compared to undigested homogenate (lanes 10 to 15). In panel B (the same blot), PrP-res, the lower bands at 29, 26, and 19 kDa are seen after PK in all samples (wt and LTβ$^{-/-}$). Minor variations in PrP-res intensities are due to loading differences (compare digested samples in lanes 1 to 6 and replicate undigested samples in lanes 10 to 15).

positive cells. These S-100 wt cells corresponded to those with pathologic PrP. Even more extensive networks of pathologic PrP were found in paraformaldehyde-perfused mice. Figure 4A shows a low-power view of S-100A detection in a typical spleen follicle from an infected CD-1 mouse. A reticulated network of strongly stained processes and cells is seen in the center of this follicle slice. Some cells at the periphery (P) are also stained, albeit less intensely. A deeper adjacent slice, stained for pathologic PrP, is seen in panel B. The pattern of staining in the germinal center is comparable in both sections, and arrows point to positive cytoplasmic extensions of the same FDC in both images. However, there was negligible accumulation of PrP in peripheral non-FDC cells. These data show that PrP accumulating cells can be positively identified as FDC.

Higher resolution of the distribution of abnormal PrP showed that PrP largely accumulated at the surface of FDC. Figure 4C shows a low-power view of PrP-positive FDC, and the arrow points to the cell that was optically sliced in Fig. 5 to show details of PrP accumulation. Figure 5 shows every second section moving from the inside of an FDC that has a typical irregular horseshoe-shaped nucleus and extends numerous irregular cytoplasmic processes (arrows, section 11). Higher-number sections sequentially move to the surface of this cell (section 21), where only the topmost plasma membrane remains. The vast majority of pathologic PrP in every slice is found at the surface of the FDC as it intimately wraps around many small round lymphocytes (L). Even without deconvolution, small, intensely stained aggregates of PrP were also ap-

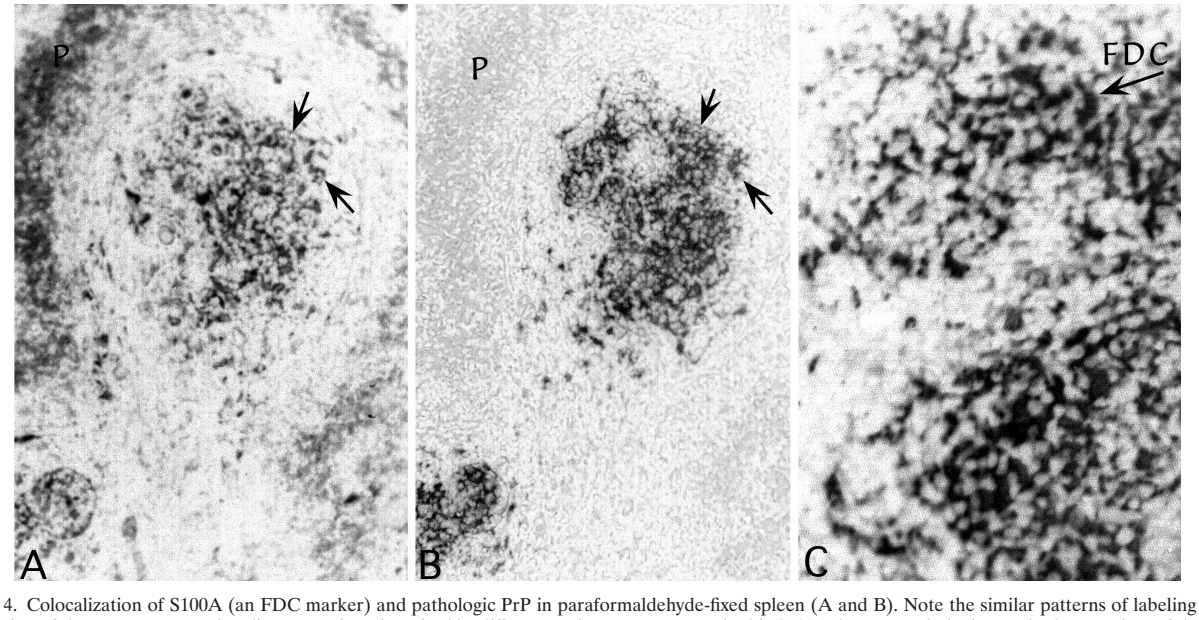

FIG. 4. Colocalization of S100A (an FDC marker) and pathologic PrP in paraformaldehyde-fixed spleen (A and B). Note the similar patterns of labeling and the continuation of the same processes in adjacent sections (required by different antigen exposure methods). S100A, but not pathologic PrP, is also seen in peripheral cells but is less intense. Panel C shows an FDC stained for pathologic PrP within a larger network that was resolved by confocal microscopy in Fig. 5. Fluorescent photos are shown inverted, and therefore unlabeled nuclei are the lightest elements. Infected CD-1 and wt mice showed comparable FDC accumulation levels on FDC.

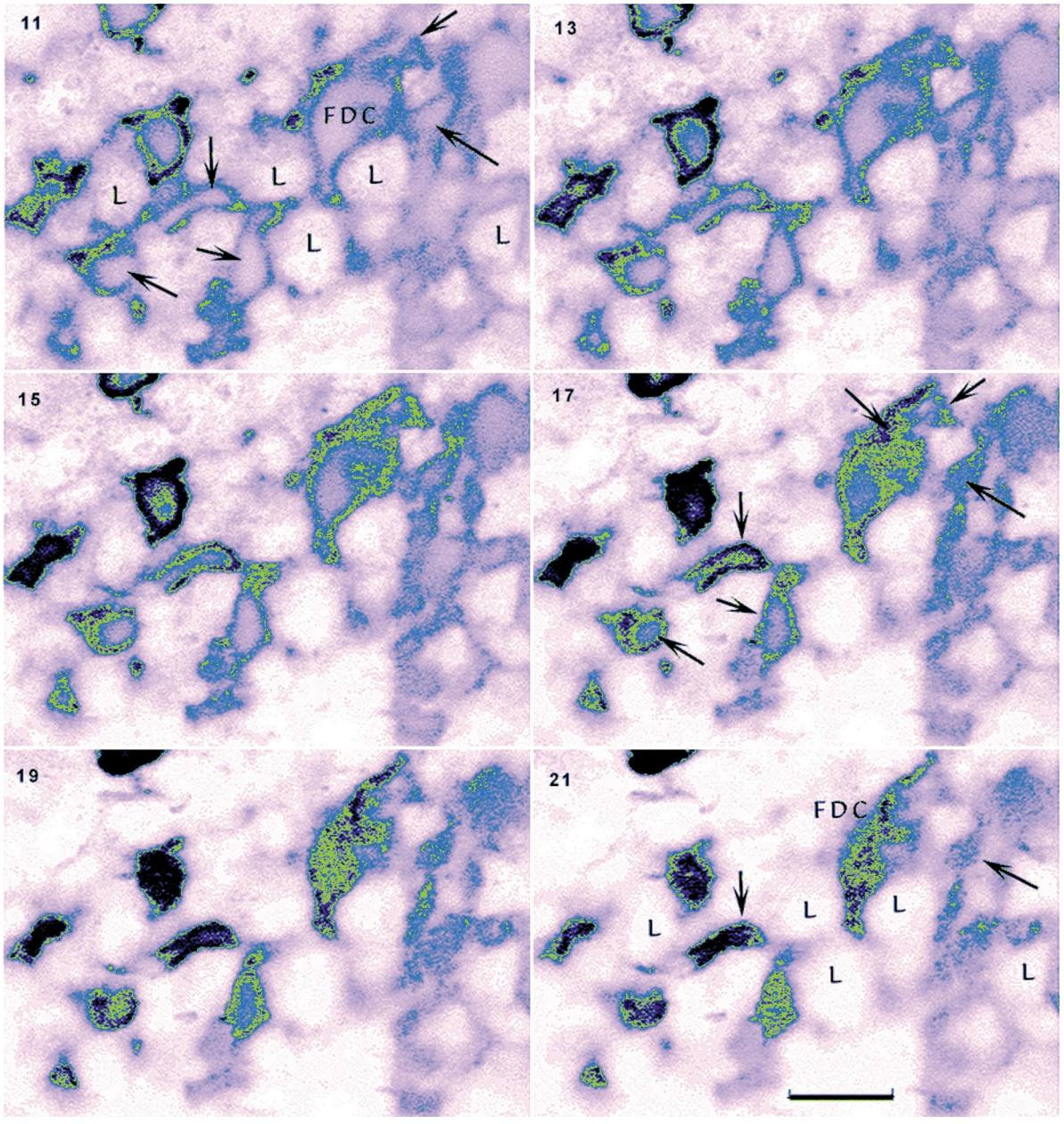

FIG. 5. Montage of an FDC starting from the center of the cell (section 11) and following the plasma membrane to its topmost surface (section 21). Every other section (from a 30-step series, each step being 50 nm) shows surface labeling of FDC processes (arrows) that invest and interdigitate around lymphocytic cells (L). The intensity of label is color coded for increasing PrP signal intensity (pink to blue to green to black). The cytoplasm of the FDC cell body and its reticular processes show a paucity of PrP. Aggregates of punctate (black) clusters of PrP are also apparent on the FDC surface (e.g., section 21). Bar, 10 μm.

parent on the surface at higher power (see slice 21). These observations demonstrate that FDC could have the capacity to both acquire and donate agent aggregated with PrP merely through surface physical contacts with other lymphocytes. In principle, this should be sufficient to modestly enhance agent dissemination.

DISCUSSION

These studies show that FDC, marginal metallophilic macrophages, and a highly organized lymphoid structure are not required for either the effective replication or the dissemination of a CJD agent administered i.p. There was only a small increase in incubation time to terminal disease at low and limiting dilutions of agent in mice verified as FDC null and lacking germinal centers. Furthermore, because i.v. and i.p. inoculations gave comparable incubation times with little variation among individual mice, it was unlikely that the reproducible spread of this CJD agent to the brain could be based only on the accidental injection of small peripheral nerves. This route was proposed for the spread of ME7 scrapie (6). Several other lines of evidence implicate hematogenous spread of agent in CJD, a route that does not necessarily exclude neural pathways. These include the original observation that white blood cells carry the infectious agent in various CJD models (20, 26, 27, 35). The perivascular lesions found here in the

cerebrum after i.p. inoculation are also most consistent with agent spread by cells traveling through the bloodstream. Based on molecular and temporal studies in this model, one of the cell types most likely to carry the agent across the blood-brain barrier is the migrating and activated microglial cell (1), a derivative of myeloid or macrophage lineage.

Macrophages would also be the most obvious cell type to disseminate agent after both i.c. and i.p. inoculation. Macrophages should be involved in initial phagocytosis of the infectious inoculum, although other cells may also bind or take up agent. Newly published depletion experiments suggest but do not prove early phagocytosis of PrP, presumably a surrogate for infectivity (3). Subsequent involvement of macrophages was supported by experiments here showing that spleen macrophages retain significant FU infectivity 8 weeks after i.p. inoculation, a time preceding substantial replication of agent in the brain and, as noted above, several different studies have demonstrated agent in splenic macrophages during clinical disease. Perpetuated macrophage infectivity could derive from local ingestion of other infected cell fragments (such as those created during apoptosis in the spleen) or might reflect a subpopulation of migrating macrophages that had originally taken up the agent in the peritoneum. Moreover, macrophages in principle could also directly invade or travel on and infect peripheral nerves to deliver agent to the CNS. Finally, macrophages can be very long-lived, and therefore these cells can act as reservoirs of infection that can be activated after a long quiescent period. Whether myeloid cells alone are sufficient for agent spread or if other lymphocytes or their products are required for agent dissemination to the brain remains to be seen.

The first demonstration of a dramatic resistance to i.p. infection was made in a more broadly immunodeficient SCID mouse model which lacked B and T cells in addition to FDC and used another (Fukuoka-1) CJD agent (16). Because pathologic PrP, often assumed to be the infectious agent, associated with FDC rather than with other lymphoid cells, it was natural to conclude that FDC were the essential sites for agent replication. Our results in a more precisely targeted mouse model do not support this view. Indeed, the paucity of pathologic PrP in the spleen and lymph nodes had surprisingly little effect on the progression of CJD at low doses. Higher doses of RML scrapie have also shown unimpeded susceptibility to peripheral infection in TNFR $1^{-/-}$ mice, another distinct transgenic line lacking FDC (17). Furthermore, in a study just published, half of the TNF$\alpha^{-/-}$ mice without FDC also developed ME7 scrapie at limiting i.p. doses (6), a finding compatible with our FU studies at a limiting dilution in LT$\beta^{-/-}$ mice. All of these transgenic studies implicate non-FDC cells and other factors of the immune system for effective peripheral agent dissemination. Minor differences among different laboratories probably arise from the use of different agent strains and transgenic models. On the other hand, FDC-PrP chimeric mice, created by BM grafting after gamma irradiation, yielded data that were incompatible with this conclusion and instead implicated a marked dependence of ME7 scrapie on PrP-expressing FDC (6). ME7 strain properties may underlie this discrepancy but, in addition, chimeric mice generated by transplantation can be more complex and less homogeneous than knockout mice. For example, long-term radiation effects and heterogeneity of uncharacterized cell populations (such as tissue-sequestered macrophages) might influence outcomes in a manner unrelated to FDC.

B cells have also been emphasized in agent replication and spread. Studies with RML scrapie strain in several types of immunodeficient mice have led to the concept that B lymphocytes are required for neuroinvasion and for clinical disease. However, 5 of 11 randomly sampled mice (including RAG-$2^{0/0}$ and μMT) inoculated i.p. showed typical scrapie pathology and high levels of infectivity in the brain (17). The importance of B cells for clinical symptoms may also be overestimated since, as shown here, clinical symptoms can be undetectable in immunologically normal mice if they are injected with limiting dilutions of agent i.p. Subsequent studies also have modified and complicated interpretations, including the suggestion that B cells might transport agent to the brain by a PrP-independent mechanism (18). Some of these conundrums are further compounded by the interactive and mutually dependent nature of the immune system cells, as well as by the still-controversial nature of the infectious agent (2). At the very least it becomes essential to discriminate more precisely the accumulation and replication of agent from each other and from pathologic PrP in different cell types.

If PrP acts as an essential molecular scaffold for the replication or propagation of these infectious agents, altered PrP could be formed and amplified as a noxious byproduct of infection (23). Moreover, in the immune system, aggregated PrP could collaborate in an inflammatory response to trap the infectious agent. Aggregates of PrP on the surface of FDC, as shown here by confocal microscopy, probably represent such traps. They may be passively deposited from other passing cells or they may be part of a more active attempt to immobilize and present the infectious agent to other lymphoid cells for clearance. In either case, the surface positioning of agent-PrP complexes would enhance agent spread to lymphoid cells through extensive physical membrane interactions. The new high-resolution data presented here also suggest that PrP-res accumulates secondarily on FDC and may not require either internal processing of PrP or agent replication within FDC. While our studies do not resolve the question of agent replication by FDC, the relative paucity of abnormal PrP within this cell type might suggest little agent replication by these cells. Interestingly, recent studies on genetic, but noninfectious, prion diseases show PrP pathology entails an endoplasmic reticulum transmembrane form of the protein that is comparable to that elicited by infection (13). These pathologic forms of PrP have also been shown to accumulate in microsomal and Golgi membranes within the cell (14). Thus, actively replicating agent would probably educe PrP accumulation at these internal sites rather than on the FDC surface. It will be of interest to determine whether PrP aggregates on the FDC surface require the presence of antibodies or whether they include antibody complexes. It is entirely possible that antibodies are excluded from the FDC surface and that trapping of agent by PrP is one way the agent evades immune recognition.

ACKNOWLEDGMENTS

This work was supported by NIH grants NS12674 and NS34569.
R.A.F. is an Investigator of the Howard Hughes Medical Institute.

REFERENCES

1. **Baker, C., Z. Y. Lu, I. Zaitsev, and L. Manuelidis.** 1999. Microglial activation varies in different models of Creutzfeldt-Jakob disease. J. Virol. **73:**5089–5097.
2. **Balter, M.** 1999. Prions: a lone killer or a vital accomplice? Science **286:** 660–662.
3. **Beringue, V., M. Demoy, C. I. Lasmezas, B. Gouritin, C. Weingarten, J.-P. Deslys, J.-P. Andreux, P. Couvreur, and D. Dormont.** 2000. Role of spleen macrophages in the clearance of scrapie agent early in pathogenesis. J. Pathol. **190:**495–502.
4. **Brown, P.** 1990. The phantasmagoric immunology of transmissible spongiform encephalopathy, p. 305–313. *In* B. Waksman (ed.), Immunologic mechanisms in neurologic and psychiatric disease. Raven Press, New York, N.Y.
5. **Brown, K., K. Stewart, M. Bruce, and H. Fraser.** 1996. Scrapie in immuno-

deficient mice, p. 159–166. *In* L. Court and B. Dodet (ed.), Transmissible subacute spongiform encephalopathies: prion diseases. Elsevier, Paris, France.
6. **Brown, K., K. Stewart, D. Ritchie, N. Mabbott, A. Williams, H. Fraser, W. Morrison, and M. Bruce.** 1999. Scrapie replication in lymphoid tissues depends on prion protein-expressing follicular dendritic cells. Nat. Med. **5:** 1308–1312.
7. **Büeler, H., A. Aguzzi, A. Sailer, R.-A. Greiner, P. Autenried, M. Auget, and C. Weissmann.** 1993. Mice devoid of PrP are resistant to scrapie. Cell **73:** 1339–1347.
8. **Caughey, B., R. E. Race, and B. Chesebro.** 1988. Detection of prion protein mRNA in normal and scrapie-infected tissues. J. Gen. Virol. **69:**711–716.
9. **Eklund, C. M., R. C. Kennedy, and W. J. Hadlow.** 1967. Pathogenesis of scrapie virus infection in the mouse. J. Infect. Dis. **117:**15–22.
10. **Fu, Y.-X., and D. Chaplin.** 1999. Development and maturation of secondary lymphoid tissues. Annu. Rev. Immunol. **17:**399–433.
11. **Gajdusek, D. C.** 1977. Unconventional viruses and the origin and disappearance of kuru. Science **197:**943–960.
12. **Hadlow, W., R. Race, and R. Kennedy.** 1987. Temporal distribution of transmissible mink encephalopathy virus in mink inoculated subcutaneously. J. Virol. **61:**3235–3240.
13. **Hedge, R., P. Tremblay, D. Groth, S. DeArmond, S. Prusiner, and V. Lingappa.** 1999. Transmissible and genetic prion diseases share a common pathway of neurodegeneration. Nature **402:**822–826.
14. **Hedge, R., J. Mastrianni, M. Scott, K. DeFea, P. Tremblay, M. Torchia, S. DeArmond, S. Prusiner, and V. Lingappa.** 1998. A transmembrane form of the prion protein in neurodegenerative disease. Science **279:**827–834.
15. **Imai, Y., and M. Yamakawa.** 1996. Morphology, function and pathology of follicular dendritic cells. Pathol. Int. **46:**807–833.
16. **Kitamoto, T., T. Muramoto, S. Mohri, K. Doh-Ura, and J. Tateishi.** 1991. Abnormal isoform of prion protein accumulates in follicular dendritic cells in mice with Creutzfeldt-Jakob disease. J. Virol. **65:**6292–6295.
17. **Klein, M., R. Frigg, E. Flechsig, A. Raeber, U. Kalinke, H. Bluethmann, F. Bootz, M. Suter, R. Zinkernagel, and A. Aguzzi.** 1997. A crucial role for B cells in neuroinvasive scrapie. Nature **390:**687–690.
18. **Klein, M., R. Frigg, A. Raeber, E. Flechsig, I. Hegyt, R. Zinternagel, C. Weissmann, and A. Aguzzi.** 1998. PrP expression in B lymphocytes is not required for neuroinvasion. Nat. Med. **4:**1429–1433.
19. **Koni, P., R. Sacca, P. Lawton, J. Browning, N. Ruddle, and R. Flavell.** 1997. Distinct roles in lymphoid organogenesis for lymphotoxins α and β revealed in lymphotoxin β-deficient mice. Immunity **6:**491–500.
20. **Kuroda, Y., C. Gibbs, H. Amyx, and D. Gajdusek.** 1983. Creutzfeldt-Jakob disease in mice: persistent viremia and preferential replication of virus in low-density lymphocytes. Infect. Immun. **41:**154–161.
21. **Manuelidis, L.** 1998. Vaccination with an attenuated CJD strain prevents expression of a virulent agent. Proc. Natl. Acad. Sci. USA **95:**2520–2525.
22. **Manuelidis, L.** 1997. Interphase chromosome positions and structure during silencing, transcription and replication, p. 145–168. *In* R. Van Driel and A. P. Otte (ed.), Nuclear organization, chromatin structure, and gene expression. Oxford University Press, Oxford, England.
23. **Manuelidis, L.** 1997. Beneath the emperor's clothes: the body of data in scrapie and CJD. Ann. Inst. Pasteur **8:**311–326.
24. **Manuelidis, L., and W. Fritch.** 1996. Infectivity and host responses in Creutzfeldt-Jakob disease. Virology **215:**46–59.
25. **Manuelidis, L., W. Fritch, and Y. G. Xi.** 1997. Evolution of a strain of CJD that induces BSE-like plaques. Science **277:**94–98.
26. **Manuelidis, E. E., E. J. Gorgacz, and L. Manuelidis.** 1978. Viremia in experimental Creutzfeldt-Jakob disease. Science **200:**1069–1071.
27. **Manuelidis, E. E., J. H. Kim, J. R. Mericangas, and L. Manuelidis.** 1985. Transmission to animals of Creutzfeldt-Jakob disease from human blood. Lancet **ii:**896–897.
28. **Manuelidis, E., and L. Manuelidis.** 1979. Clinical and morphological aspects of transmissible Creutzfeldt-Jakob disease. Prog. Neuropathol. **4:**1–26.
29. **Manuelidis, L., and E. Manuelidis.** 1983. Fractionation and infectivity studies in Creutzfeldt-Jakob disease. Banbury Rep. (Cold Spring Harb.) **15:** 399–412.
30. **Manuelidis, L., G. Murdoch, and E. E. Manuelidis.** 1988. Potential involvement of retroviral elements in human dementias. Ciba Found. Symp. **135:** 117–134.
31. **Manuelidis, L., T. Sklaviadis, A. Akowitz, and W. Fritch.** 1995. Viral particles are required for infection in neurodegenerative Creutzfeldt-Jakob disease. Proc. Natl. Acad. Sci. USA **11:**5124–5128.
32. **Prusiner, S.** 1995. The prion diseases. Sci. Am. **272:**30–37.
33. **Prusiner, S. B.** 1991. Molecular biology of prion diseases. Science **252:** 1515–1522.
34. **Raeber, A., M. Klein, R. Frigg, E. Flechsig, A. Aguzzi, and C. Weissmann.** 1999. PrP-dependent association of prions with splenic but not circulating lymphocytes of scrapie-infected mice. EMBO J. **18:**2702–2706.
35. **Tateishi, J.** 1985. Transmission of Creutzfeldt-Jakob disease from human blood and urine into mice. Lancet **ii:**1074.
36. **Tateishi, J., H. Nagara, K. Hikita, and Y. Sato.** 1984. Amyloid plaques in the brains of mice with Creutzfeldt-Jakob disease. Ann. Neurol. **15:**278–280.
37. **Tsunoda, T., M. Yamakawa, and T. Takahashi.** 1999. Differential expression of Ca^{2+}-binding proteins on follicular dendritic cells in non-neoplastic and neoplastic lymphoid follicles. Am. J. Pathol. **155:**805–814.